

Multiple periods in the variability of the supermassive black hole binary candidate quasar PG1302-102?

M. Charisi,^{1*} I. Bartos,² Z. Haiman,¹ A. M. Price-Whelan,¹ S. Márka²

¹*Department of Astronomy, Columbia University, New York, NY 10027, USA*

²*Department of Physics, Columbia University, New York, NY 10027, USA*

5 September 2018

ABSTRACT

[Graham et al. 2015](#) discovered a supermassive black hole binary (SMBHB) candidate and identified the detected 5.2 yr period of the optical variability as the orbital period of the binary. Hydrodynamical simulations predict multiple periodic components for the variability of SMBHBs, thus raising the possibility that the true period of the binary is different from 5.2 yr. We analyse the periodogram of PG1302 and find no compelling evidence for additional peaks. We derive upper limits on any additional periodic modulations in the available data, by modeling the light-curve as the sum of red noise and the known 5.2 yr periodic component, and injecting additional sinusoidal signals. We find that, with the current data, we would be able to detect with high significance (false alarm probability $< 1\%$) secondary periodic terms with periods in the range predicted by the simulations, if the amplitude of the variability was at least ~ 0.07 mag (compared to 0.14 mag for the main peak). A three-year follow-up monitoring campaign with weekly observations can increase the sensitivity for detecting secondary peaks $\approx 50\%$, and would allow a more robust test of predictions from hydrodynamical simulations.

1 INTRODUCTION

It is well established that massive galaxies harbour supermassive black holes in their centres, with masses tightly correlated with global properties of the host galaxy ([Kormendy & Ho 2013](#)). According to cosmological models of hierarchical structure formation, galaxies grow through frequent mergers ([Springel, Di Matteo & Hernquist 2005](#); [Robertson et al. 2006](#)). The formation of supermassive black hole binaries (SMBHB) is a natural consequence of the above process. Combining the high expected rates of galaxy mergers with the expectation that SMBHBs spend a large fraction of their lifetimes at close separation ([Haehnelt & Kauffmann 2002](#)), SMBHBs at sub-parsec separations should be fairly common, despite the scarcity of observational evidence.

Recently, [Graham et al. \(2015, hereafter G15\)](#) reported the detection of strong periodic variability in the optical flux of quasar PG1302-102. PG1302 is a bright (median V-band magnitude ~ 15), radio-loud quasar at redshift $z = 0.2784$, with inferred black hole (BH) mass of $10^{8.3-9.4} M_{\odot}$. The light curve in optical bands shows a quasi-sinusoidal modulation, with a best-fit period of (5.2 ± 0.2) yr and amplitude of ≈ 0.14 mag. G15 suggest that PG1302 may be a SMBHB at close separation (~ 0.01 pc), interpreting the observed periodicity as the (redshifted) orbital period of the binary.

Theoretical work on circumbinary disks predicts that SMBHBs can excite periodic enhancements of the mass accretion rate that could translate into periodic luminosity enhancements, not only at the orbital period, but also on longer and shorter timescales. More specifically, if the binary

is embedded in a thin disk, the gas will be expelled from the central region due to torques exerted by the binary, creating a cavity ([Artymowicz & Lubow 1994](#)). Several hydrodynamical simulations ([Hayasaki, Mineshige & Sudou 2007](#); [MacFadyen & Milosavljević 2008](#); [Noble et al. 2012](#); [Shi et al. 2012](#); [Roedig et al. 2012](#); [D’Orazio, Haiman & MacFadyen 2013](#); [Farris et al. 2014](#)) indicate that the interaction of the individual BHs with the inner edge of the accretion disk can pull gaseous streams into the cavity, resulting in periodic modulation of the accretion rate at timescales corresponding to $\approx 1/2$ and 1 times the binary’s orbital period. For high BH mass ratios ($q \equiv M_1/M_2 \gtrsim 0.3$), the cavity is lopsided, leading to the formation of a hotspot in the accretion disk. The strongest modulation in the accretion rate is observed at the orbital period of the overdense region, a few ($\sim 3-8$) times the orbital period of the binary.

These results imply that the observed 5.2 yr period in PG1302 may not reflect the orbital period of the binary. If the orbital period of the binary is shorter/longer than the period of optical variability (hereafter, optical period, t_{opt}), there are major implications for the expected quasars binary fraction, and the probability of detecting SMBHBs ([Haiman, Kocsis & Menou 2009](#)), as well as the physics of the orbital decay. [D’Orazio et al. \(2015\)](#) showed that, under the assumption that the optical period corresponds to the longer period of the hotspot in the accretion disk, PG1302 would be in the gravitational inspiral regime. This would confirm that SMBHBs can produce bright electromagnetic

emission even at these late stages of the merger (Noble et al. 2012; Farris et al. 2015).

The significance of the above considerations motivates us to search for multiple periodicity in the optical variability of PG1302. In this paper, we search for secondary peaks in the Lomb-Scargle periodogram. We assess the statistical significance of the identified peaks by generating mock time series that show correlated noise, as expected for quasars (Kelly, Bechtold & Siemiginowska 2009). The false alarm probability of the most significant secondary peak identified in our analysis is 6%, below a reliable detection threshold. We set upper limits on the amplitude of secondary sinusoid variations that could be detectable with high significance, in the presence of correlated noise, as well as the already known 5.2 yr periodic signal. Although the current data do not allow the detection of weak secondary periodic terms, the addition of three years of observations, can improve the sensitivity up to a factor of 2, lowering the detection threshold to ~ 0.04 mag.

2 DATA ANALYSIS

We investigate the possibility of multiple periodic terms in the photometric variability of PG1302 by analysing the light curve published in G15¹. The light curve consists of data from: (1) the Catalina Real-time Transient Survey (telescopes CSS and MLS; Drake et al. 2009; Mahabal et al. 2011); (2) the Lincoln Near-Earth Asteroid Research (LINEAR; Sesar et al. 2011) program; (3) the All Sky Automated Surveys (ASAS; Pojmanski 1997) and; (4) other archival data (Garcia et al. 1999; Eggers, Shaffer & Weistrop 2000), providing a baseline of ~ 20 yr. The different datasets were calibrated to account for the differences between the various photometric systems, as detailed in G15.

For our analysis, we use the generalised version of the Lomb-Scargle (LS) periodogram (Lomb 1976; Scargle 1982; Zechmeister & Kürster 2009), a standard method for detecting periodicity in unevenly sampled time series². We compute the periodogram for 1000 trial frequencies on a uniform logarithmic grid, spanning from $f_{min} = 1/T_{data}$ to $f_{max} = 1/(2\Delta T)$, where T_{data} is the baseline of the light curve and ΔT is the median time interval between successive data points.

For each peak in the periodogram, we then calculate the probability that a peak of equal power can arise by chance (false alarm probability; hereafter FAP). For this purpose, we generate mock time series that mimic the optical variability of PG1302. Quasars show correlated stochastic variability, best described as a damped random walk (Kelly, Bechtold & Siemiginowska 2009). At high frequencies, the power spectral density decreases with frequency ($PSD \sim 1/f^2$, or red noise), whereas, at low frequencies, it becomes flat ($PSD \sim f^0$, or white noise). Furthermore, PG1302 exhibits strong sinusoidal variability with period of $1,884 \pm 88$ d (identified by wavelet and autocorrelation function (ACF)

¹ We are grateful to M. Graham for providing us with their calibrated photometric data in electronic form.

² Throughout the analysis, we make use of the astroML python package (Vanderplas et al. 2012; Ivezić et al. 2014).

based techniques as detailed in G15) and amplitude of 0.14 mag.

We first identify the best-fit model for PG1302 as follows. We generate evenly sampled stochastic time series with a dense temporal resolution ($dt = 2$ h) and peak-to-peak amplitude A , and with a power spectrum $\sim 1/f^2$ (Timmer & Koenig 1995). We add a sine wave, with properties as in G15, and subsample to match the observation times in the light curve of PG1302. We calculate the average LS periodogram from 50 realisations. Next, we subtract this periodogram from the observed LS periodogram of PG1302 and calculate the residuals. We repeat the above process, varying the amplitude A between 0.5 to 2 times the peak-to-peak amplitude of the light curve ($m_{max} - m_{min}$) of PG1302, and determine the amplitude A that minimises the residuals.

With the best-fit amplitude A , we generate 10,000 realisations of red noise with periodic variability, as before, and calculate the LS periodogram for each realisation. At each trial frequency, we calculate the FAP by comparing the power in the PG1302's periodogram to the distribution of power at the same frequency in the periodograms of the mock time series. We define FAP_f , the false alarm probability *per frequency* as the fraction of the 10,000 simulated periodograms with power exceeding the value observed for PG1302.

Based on the results from hydrodynamical simulations discussed above, we search for secondary peaks around the main 5.2 yr peak, i.e. between $(f_{min}, f_{max}) = (2.37, 3.8)$ nHz and $(9.5, 92)$ nHz³. The frequency ranges together contain a total of $N_{tot} = 526$ frequency bins. Since these bins have non-trivial correlations, we compute the effective number of independent bins, N_{eff} , for each FAP_f , by: (i) applying the same analysis as above, but replacing the PG1302 data with each individual simulated mock periodogram, and (ii) determining the fraction of the 10,000 mock periodograms that show FAP_f (or lower) at *any* frequency between $f_{min} \leq f \leq f_{max}$. For $FAP_f = 10^{-4}$, we find $N_{eff} = 80$, and the total $FAP \equiv N_{eff} \times FAP_f = 0.008$.⁴

3 RESULTS

If the optical variability of PG1302 is the superposition of multiple periodic terms, it is expected that significant secondary peaks will appear in the periodogram. Moreover, following the predictions of hydrodynamical simulations, we expect the peaks roughly at ratios 1:2 (1 and 1/2 times the orbital period) or from 1:3:6 to 1:8:16 (hotspot period, orbital period and half of the orbital period of the binary).

More specifically, with the limitations imposed by the currently available data, we were able to explore three possibilities: (A) If the optical period t_{opt} is the binary orbital period t_{bin} , is there a secondary peak near $0.5t_{bin}$? (B) If t_{opt} is $0.5t_{bin}$, is there a periodic component at t_{bin} ? (C) If t_{opt} is the long orbital period $\approx (3-8)t_{bin}$ of the hotspot in the disk, as hypothesised by D'Orazio et al. (2015), is there a secondary period corresponding to $\approx 0.5t_{bin}$ or t_{bin} ? Note that in scenario (A), periodicity is predicted at $\sim (3-8)t_{bin}$.

³ These ranges are illustrated by the shaded areas in Fig. 3

⁴ N_{eff} is decreased to ≈ 60 and ≈ 30 for $FAP_f = 10^{-3}$ and $FAP_f = 10^{-2}$, respectively.

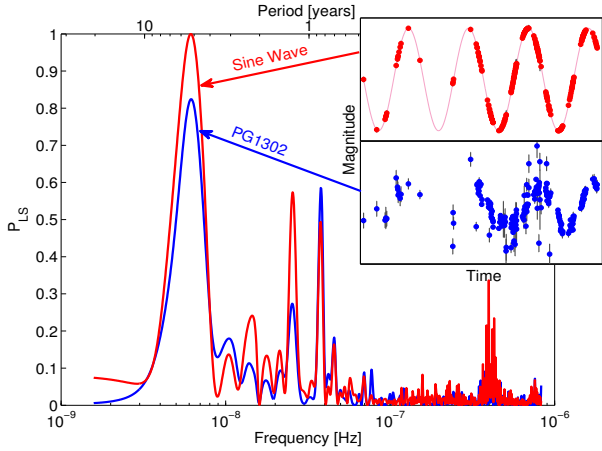


Figure 1. LS periodogram of PG1302 (blue) and of a sine wave sampled at the observation times of PG1302 (red). The embedded plots illustrate the respective light curves, spanning a baseline of ~ 20 yr. The irregular sampling of the data produces the artificial secondary peaks seen in the red curve.

However, the 20-yr baseline of the light curve does not allow us to probe this low-frequency range.

The detection of weaker periodic terms in the presence of a known significant periodic component is in general challenging. The periodogram of an unevenly sampled time series is the convolution of the actual power spectrum of the signal and the window function, defined by the irregular time sampling. A periodic signal can introduce aliasing peaks, and hide the secondary peaks. To illustrate this, in Fig. 1, we show the LS periodogram of PG1302, superimposed with the periodogram of a pure sine wave, with period of 5.2 yr, sampled at the observation times of PG1302. The periodogram of the sine wave shows a set of artificial secondary aliasing peaks, which coincide with many of the observed features in the periodogram of PG1302.⁵

We analysed the LS periodogram of PG1302 searching for secondary peaks, focusing on the frequencies of interest, within a factor of ~ 10 around the peak of the main period. We assessed the statistical significance of the observed secondary peaks using the method discussed in § 2 above. In Fig. 2, we present the periodogram of PG1302 with the average and the maximum periodogram power from 10,000 realisations of the simulated variability, with the latter corresponding to our $FAP=1\%$ significance threshold. In the bottom panel, we show both FAP_f and the total FAP at each frequency. We identify a secondary peak at ~ 40 nHz (~ 300 d), with the lowest FAP (< 0.008). This peak is most likely artificial, since it coincides with one of the strongest aliasing peaks demonstrated in Fig. 1. The most significant peak that does not overlap with aliasing peaks appears at ~ 77.5 nHz (~ 155 d), with a $FAP=0.06$ ($FAP_f=0.001$).

We next derive upper limits for putative secondary periodic terms with the current data. For this purpose, we simulate time series as before, but with an additional sine wave component. We identified the minimum amplitude of the second component at which the power in the new peak

⁵ The aliasing peaks are predictable, and could be used to better determine the amplitude and frequency of the 5.2 yr peak.

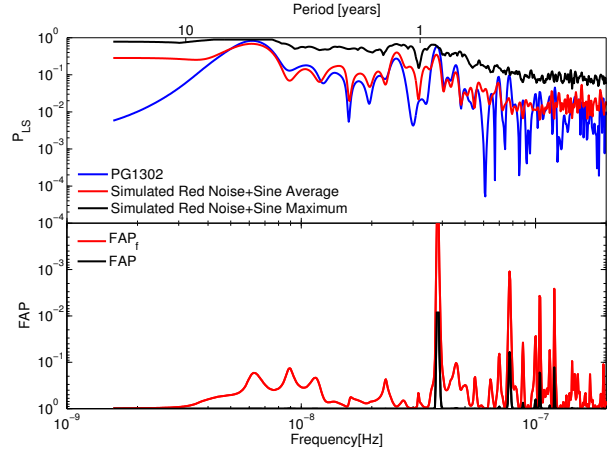


Figure 2. *Top panel:* LS periodogram of PG1302 (blue), superimposed with the average of 10,000 realisations of a model that includes stochastic red noise and a 5.2 yr-sinusoid. The maximum power among these 10,000 realisations is also shown (black), corresponding to 1% false alarm probability threshold. *Bottom panel:* False alarm probability per frequency (red) and total FAP (black) of PG1302's periodogram, as a function of frequency. Note that the y -axis in the bottom panel decreases upwards.

in the LS periodogram exceeded the $FAP < 1\%$ detection threshold at least 90% of the time. We repeated this process for different frequencies within the factor of 10 range of interest. In Fig. 3, we present the minimum relative amplitude (corresponding also to V-band magnitude) of a secondary sinusoid that would be detectable at different frequencies. The shaded areas in this figure indicate frequencies relevant to the three possibilities (A)-(C) discussed above.

As Fig. 3 shows, we can set weak limits for scenario (A); a second periodic component would need a higher amplitude than the one identified in G15 to be detectable. The reduced sensitivity in this frequency range is reasonable, since the light curve is well sampled only in the last ~ 9 yr, hindering the detection of a ~ 10 yr period. Moreover, at this frequency range the effect of the red noise is significant. For scenario (B) and for the majority of frequencies relevant to scenario (C), the secondary term needs to have amplitude comparable to the main 5.2 yr modulation to be detectable. Finally, for a few specific frequencies relevant to scenario (C), we can probe secondary sinusoids with amplitudes down to 25% of the amplitude of the main sinusoid (~ 0.04 mag). For the peak with the lowest FAP (155 d), the minimum detectable amplitude would be 50% of the main sinusoid (0.07 mag).

4 DISCUSSION

4.1 Quasar variability models

We have thus far modelled the variability of PG1302 using a fixed power spectrum $1/f^2$. Since quasar variability is described by a damped random walk (i.e. with the power spectrum flattening at low frequencies), white (or pink) noise may describe the quasar variability more accurately at low frequencies. To assess how this impact our conclusions, we repeated the analysis described above but with stochastic noise exhibiting $1/f$ (pink noise) and flat (white

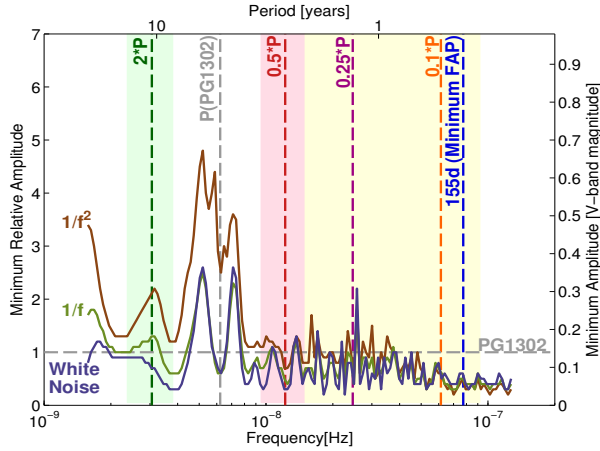


Figure 3. The minimum amplitude of a secondary sinusoid term that would be detectable at each frequency. The y axis shows the amplitude relative to that of the main 5.2 yr peak (left), and also in V mag (right). The three curves correspond to noise models with three different power-law power spectra: $\propto 1/f^2$ (brown), $\propto 1/f$ (olive), and constant white noise (dark blue). Frequency ranges relevant to different scenarios are highlighted with light pink (A), light green (B) and light yellow (C). Vertical lines mark specific frequencies of interest (see text).

noise) power spectra. Our conclusions remain unchanged for these different noise models. More specifically, we identify the same peak at ~ 40 nH (~ 300 d), which we discard as aliasing with $\text{FAP} < 1\%$ both for white and pink noise; we also find the peak at ~ 77.5 nH (~ 155 d) with $\text{FAP} = 0.2$ and 0.1 for pink and white noise, respectively. The upper limits for the different noise models are also shown in Fig. 3. For white noise, the minimum detectable amplitude is almost constant (~ 0.08 mag) for all frequencies, but with fluctuations caused by the irregular sampling similarly to the red noise case. The results are again similar for pink noise, with the sensitivity falling in-between the red and white noise cases.

4.2 Historic Data

Historic photometry of PG1302 is available from the digitisation of old photographic plates, as part of the Digital Access to a Sky Century @ Harvard (DASCH; Grindlay et al. 2009) project. The measurements were in unfiltered B photographic magnitude, which is close to wide-band Johnson B magnitude and were calibrated with the AAVSO APASS catalog (Henden et al. 2012). We extracted the B-band light curve from the online database⁶ and excluded measurements with high astrometric errors or with magnitudes within 0.5 of the limiting magnitude, and data points that were flagged as plate defects. We analysed the periodogram, as before, assuming red noise variability (without the periodic component) and finding the best-fit model.

In Fig. 4, we present the B-band light curve and the LS periodogram, along with the average and maximum power of the LS periodogram from 10,000 realisations of red noise. All of the identified peaks (including the 5.2 yr period from G15)

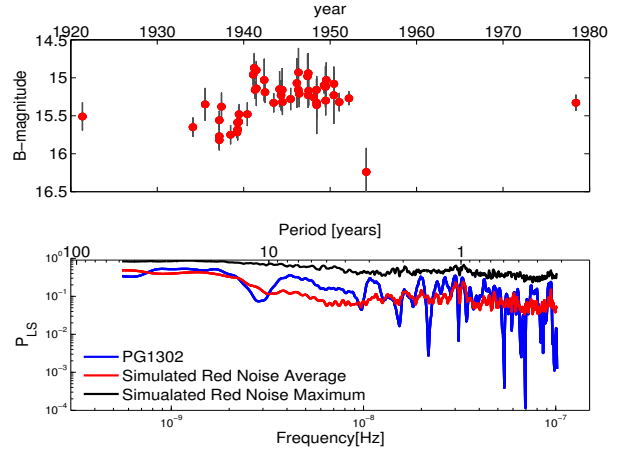


Figure 4. *Top Panel:* B-band light curve of PG1302 from the DASCH project. *Bottom Panel:* LS periodogram of the B-band light curve (blue), superimposed with the average best fit $1/f^2$ noise model (red) and the maximum power of the periodogram from 10,000 realisations of the noise (black), which corresponds to our significance threshold.

are below the significance threshold. This result, however, must be viewed in light of the photometric accuracy of the DASCH dataset. The average photometric error is 0.18 mag, exceeding the 0.14 mag amplitude of the periodic variability in G15. Interestingly, the two most significant peaks, within the interval of interest, are observed at similar frequencies (~ 42 nH and ~ 76 nH) as the peaks in the periodogram from the G15 data, although their significance remains low.

4.3 Future Data

We investigated how the sensitivity for detection of secondary peaks would increase with three years of weekly follow-up observations. In order for PG1302 to be observable throughout the year, a network of telescopes is required (e.g., Las Cumbres Observatory⁷). Given that PG1302 is a bright quasar, even small telescopes can observe it with relatively small photometric errors. To allow for a flexible, realistic (affected by weather conditions, resources etc.) observation schedule as well as to avoid strong aliasing from an exactly periodic time sampling, we generate a hypothetical follow-up data set, consisting of one randomly chosen day each week, and allowing an additional scatter of ± 3 h in the observation times. We also assume photometric errors of 10 mmag, comparable to the ones in G15.

We analyse the extended light curve as before: we generate 10,000 time series that exhibit red noise variability with a periodic component as in G15, sampled at the observation times (including both the existing and future data) and calculate the LS periodogram. We set our significance threshold to the maximum power of the periodogram from the 10,000 realisations ($\text{FAP} \leq 1\%$). Next, as done above, we include a secondary sinusoidal term and identify the minimum amplitude that would result in a peak with power above the threshold 90% of the time.

⁶ <http://dasch.rc.fas.harvard.edu/lightcurve.php>

⁷ <http://lco.net/>

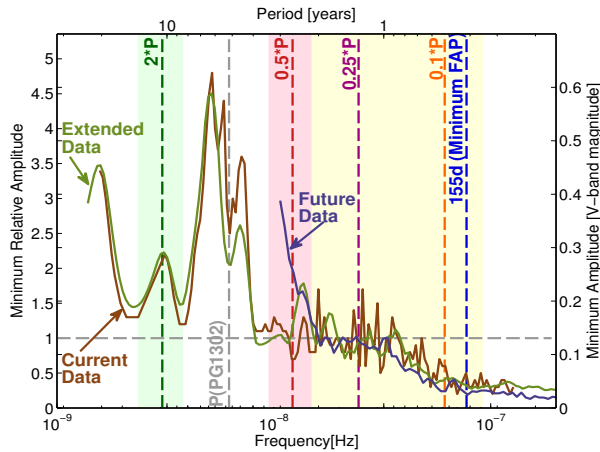


Figure 5. Minimum relative amplitude (also in V mag) of a secondary sinusoid versus frequency of secondary sinusoid that could be detectable in the current data (brown), in data extended with three years of weekly follow-up observations (olive) and in three years of future data only (dark blue). The shaded regions show the frequencies of interest, with color coding as before.

Fig. 5 shows the upper limits for detection with the extended data, compared to the upper limits with only the current data. For low frequencies (e.g., scenarios (A) and (B)), the sensitivity does not improve with the addition of three-years of data. A longer monitoring campaign is required for this purpose. For frequencies relevant to scenario (C), the improvement varies from marginal to a factor of 2, depending on the precise frequency. Furthermore, we calculate upper limits based only on the future data and find that the sensitivity for detection of a secondary term can reach as low as 20% of the amplitude of the main component (~ 0.03 mag) at some frequencies. This suggests that a multi-year follow-up with frequent sampling, by itself, could significantly improve the sensitivity to detect high-frequency (~ 1 yr) peaks;

4.4 Implications for SMBH Binary Models

The lack of a significant secondary peak can place constraints on the physical parameters of the SMBHB PG1302. In particular, models that predict two peaks, comparable in height, and separated in frequency by a factor of few, can be ruled out. While this is not a generic prediction of hydrodynamical simulations, for specific mass ratios within the range of $0.25 < q < 0.45$, two near-equal peaks are predicted in the periodograms of the mass accretion rate onto the BHs Farris et al. (2014, see their Fig. 9). The specific value of the disfavoured ratio q depends on disk parameters (viscosity, temperature) - and also on how one defines the accretion rate. If the accretion rate is defined based on the total mass accreting into the central cavity, this q value would be somewhat above $q = 0.5$ (see Fig. 6 in D’Orazio, Haiman & MacFadyen 2013).

5 CONCLUSIONS

The presence of multiple periodic components in the variability of SMBHBs is predicted by hydrodynamical simula-

tions of circumbinary disks. The detection of multiple periodicity would provide additional indication that PG1302 is a SMBHB. We analysed the LS periodogram of the optical light-curve of the SMBHB candidate quasar PG1302 to search for multiple periodic components, and assessed the statistical significance of secondary peaks by simulating the variability of PG1302. Our analysis returned a peak with FAP=6%, below our detection threshold. By injecting fake secondary sinusoids into our models, we found that the current data would only allow the detection of secondary periodic modulations comparable in amplitude to the main peak. Future observations (for a few years, at weekly sampling), and/or a more sophisticated analysis, which can mitigate the effects of aliasing, could significantly improve the detection capability and help uncover secondary peaks expected to be produced by SMBH binaries.

REFERENCES

- Artymowicz P., Lubow S. H., 1994, ApJ, 421, 651
D’Orazio D. J., Haiman Z., Duffell P., Farris B. D., MacFadyen A. I., 2015, MNRAS, submitted
D’Orazio D. J., Haiman Z., MacFadyen A., 2013, MNRAS, 436, 2997
Drake A. J. et al., 2009, ApJ, 696, 870
Eggers D., Shaffer D. B., Weistrop D., 2000, AJ, 119, 460
Farris B. D., Duffell P., MacFadyen A. I., Haiman Z., 2014, ApJ, 783, 134
Farris B. D., Duffell P., MacFadyen A. I., Haiman Z., 2015, MNRAS, 447, L80
Garcia A., Sodr e L., Jablonski F. J., Terlevich R. J., 1999, MNRAS, 309, 803
Graham M. J. et al., 2015, Nature, in press, e-print ArXiv:1501.01375
Graham M. J. et al., 2015, Nature, 518, 74
Grindlay J., et al., 2009, in ASP Conf. Series, Vol. 410, Preserving Astronomy’s Photographic Legacy: Current State and the Future of North American Astronomical Plates, Osborn W., Robbins L., eds., p. 101
Haehnelt M. G., Kauffmann G., 2002, MNRAS, 336, L61
Haiman Z., Kocsis B., Menou K., 2009, ApJ, 700, 1952
Hayasaki K., Mineshige S., Sudou H., 2007, PASJ, 59, 427
Henden A. A., Levine S. E., Terrell D., Smith T. C., Welch D., 2012, Journal of the American Association of Variable Star Observers (JAAVSO), 40, 430
Ivezi c  ., Connolly A., Vanderplas J., Gray A., 2014, Statistics, Data Mining and Machine Learning in Astronomy. Princeton University Press
Kelly B. C., Bechtold J., Siemiginowska A., 2009, ApJ, 698, 895
Kormendy J., Ho L. C., 2013, ARA&A, 51, 511
Lomb N. R., 1976, Ap&SS, 39, 447
MacFadyen A. I., Milosavljevi c M., 2008, ApJ, 672, 83
Mahabal A. A. et al., 2011, Bulletin of the Astronomical Society of India, 39, 387
Noble S. C., Mundim B. C., Nakano H., Krolik J. H., Campanelli M., Zlochower Y., Yunes N., 2012, ApJ, 755, 51
Pojmanski G., 1997, Acta Ast., 47, 467
Robertson B., Bullock J. S., Cox T. J., Di Matteo T., Hernquist L., Springel V., Yoshida N., 2006, ApJ, 645, 986

- Roedig C., Sesana A., Dotti M., Cuadra J., Amaro-Seoane P., Haardt F., 2012, *A&A*, 545, A127
- Scargle J. D., 1982, *ApJ*, 263, 835
- Sesar B., Stuart J. S., Ivezić Ž., Morgan D. P., Becker A. C., Woźniak P., 2011, *AJ*, 142, 190
- Shi J.-M., Krolik J. H., Lubow S. H., Hawley J. F., 2012, *ApJ*, 749, 118
- Springel V., Di Matteo T., Hernquist L., 2005, *MNRAS*, 361, 776
- Timmer J., Koenig M., 1995, *A&A*, 300, 707
- Vanderplas J., Connolly A., Ivezić Ž., Gray A., 2012, in *Conference on Intelligent Data Understanding (CIDU)*, pp. 47–54
- Zechmeister M., Kürster M., 2009, *A&A*, 496, 577